Soil & Tillage Research 229 (2023) 105659

Contents lists available at ScienceDirect

Soil & Tillage Research

journal homepage: www.elsevier.com/locate/still

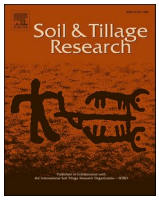

Glyphosate and AMPA dynamics during the transition towards conservation agriculture: Drivers under shallow groundwater conditions

Marta Mencaroni [a], Matteo Longo [a,*], Alessandra Cardinali [a], Barbara Lazzaro [b], Giuseppe Zanin [a], Nicola Dal Ferro [a], Francesco Morari [a]

[a] Department of Agronomy, Food, Natural Resources, Animals and Environment, Agripolis, University of Padova, Viale Dell'Università 16, 35020 Legnaro, Padova, Italy
[b] Regione Del Veneto, Direzione Agroambiente, Caccia e Pesca, U.O. Agroambiente, Via Torino 110, Mestre, VE, Italy

ARTICLE INFO

Keywords:
Solute transport
Freundlich isotherms
Soil profile
Oxides

ABSTRACT

The environmental fate of glyphosate and its metabolite AMPA were investigated in buried lysimeters in a factorial combination of two cropping systems (conservation and conventional agriculture) and two water table depths (120 and 60 cm). Glyphosate was applied at a rate of 1.44 kg ha^{-1} a.i., and pore-water was sampled for 48 non-consecutive days along the soil profile (15, 30 and 60 cm) as well as the groundwater. Glyphosate and AMPA concentration in soil was detected to compare the effect of different soil-crop managements on transformation/dissipation dynamics and a full characterization of the soil profile was performed. Freundlich adsorption coefficients were calculated down to 110 cm depth and correlated to laboratory-estimated soil properties. Clay minerals, soil organic carbon, phosphate content, Al and Fe amount were the driving factors influencing most of the glyphosate sorption, regardless of the crop and water management system that did not differentiate between adsorption dynamics. In contrast, conservation practices differently affected glyphosate concentration in the soil profile, although its adoption was limited to two years. Moreover, the occurrence of a shallow water table influenced glyphosate transport in the vadose zone, and its detection in groundwater supported the hypothesis of fast transport of the molecule as mediated by preferential pathways, compromising groundwater quality, especially in agricultural lands. On the contrary, AMPA has never been detected in the groundwater, giving evidence of a diverse adsorption and transport dynamic compared to glyphosate.

1. Introduction

The application of glyphosate-based products for weed control is strongly debated due to its extensive use in agricultural lands over several decades. Although concerns have arisen about the risk of soil and water contamination and their impact on human health, analysts have estimated that the glyphosate (GLP) market is likely to increase further, with an expected annual growth rate for herbicide sales of around 6% towards 2024, in Europe and worldwide (Antier et al., 2020). Some authors have highlighted that a possible driver of the growing use in croplands is the expansion of GLP-relying conservation agriculture (CA) practice (Benbrook, 2016), which is often supported through agri-environmental schemes as in the case of Europe. The use of GLP-based products in CA is fundamental to produce a clean seedbed before sowing. However, the investigation of GLP fate under reduced tillage conditions and its comparison with conventional practices is becoming crucial, particularly in European agroecosystems where the use of CA has been traditionally weak among farmers (Basch et al., 2015; Dal Ferro et al., 2020). In this context, still few studies have compared the effect of CA on GLP fate in soil with conventional practices. For example, Prata et al. (2005) observed a faster GLP mineralization in the no-till compared to conventional ones (DT_{50} was 14.5 and 25.8 days, respectively), whereas Carretta et al. (2021a) and Okada et al. (2019) did not find any difference in GLP dissipation time between the two systems. These results highlight that knowledge of the potential influence of CA on GLP dynamics under peculiar soil conditions in different climatic areas is still lacking.

Being a post-emergence herbicide, the fraction of GLP not intercepted by weeds may be blocked by crop residues (Khalil et al., 2018), thus impeding subsequent infiltration to soil (Locke et al., 2005). However, the positive impact of these mechanisms on pollution control was recently downplayed by Silburn (2020). The fraction of GLP that reaches the soil surface can be absorbed, degraded by soil biota, or transported through the soil matrix. In soil, GLP is considered immobile

* Corresponding author.
E-mail address: matteo.longo.2@unipd.it (M. Longo).

https://doi.org/10.1016/j.still.2023.105659
Received 28 May 2022; Received in revised form 30 January 2023; Accepted 6 February 2023
Available online 10 February 2023

or of low mobility (EFSA, 2015) due to its generally high sorption affinity to soil particles. Soil properties such as pH, texture, soil organic matter, phosphate content, soil mineralogy and exchangeable cations (Gimsing and Borggaard, 2002; Morillo et al., 2000; Okada et al., 2016; Ololade et al., 2014; Sprankle et al., 1975) can affect the sorption properties of both GLP and AMPA. In their extensive work, Sidoli et al. (2016) identified pH, available P and amorphous Fe and Al oxide contents as the most important predicting factors of GLP and AMPA adsorption constants.

In soil, besides the adsorption mechanism, GLP is mainly transformed into aminomethylphosphonic acid (AMPA), which has low mobility but high persistence. The dissipation time (DT_{50}) for GLP varies widely from a few days up to 8 months (Bento et al., 2016; Laitinen, 2009; Mencaroni et al., 2022), while for AMPA it can be even years (U.S. EPA, 1993), according to different soils and weather conditions. However, both GLP and AMPA are also highly soluble (10.5 and 1466.5 g l^{-1}), highlighting their affinity to the water phase and, in turn, increasing the risk to reach the groundwater.

The presence of GLP and AMPA in groundwater has often been detected in the past years (Carretta et al., 2021b), mainly through macropore-mediated (Kjær et al., 2011) or colloid-facilitated transport (de Jonge et al., 2004) in the soil matrix. Many authors indicated a shallow water table as a critical factor contributing to the risk of pesticide contamination of groundwater resources, especially in agricultural areas (Haarstad and Ludvigsen, 2007; Lutri et al., 2020). Shallow groundwater can enhance preferential flow pathways in the soil matrix by reducing the flow path of the solute and by modifying the flow field, thus compromising the groundwater quality (Mencaroni et al., 2021). This pathway could be emphasized under CA, where undisturbed soil structure is mostly maintained and large biopores (e.g., earthworms and roots) can facilitate the deep transport of contaminants. For this purpose, Okada et al. (2014) suggested that in clayey soils (clay >35%) under CA practices, the well-preserved soil structure might lead to an increase in the risk of leaching of chemicals. For instance, Cueff et al. (2020) found, through laboratory leaching experiments, that the protective action towards groundwater provided by the high contaminant sorption of CA soils can be offset by a high degree of preferential flow, most likely due to greater continuity of vertically oriented macropores (Wahl et al., 2004). All these phenomena can be particularly relevant in the low-lying Venetian plain of north-eastern Italy, an area where conservation agriculture practices have been recently introduced and are increasingly used in soils characterized by shallow groundwater conditions (Camarotto et al., 2018). In this area, results from previous studies suggested an increased risk of groundwater contamination in well-structured soils combined with GLP and AMPA accumulation in the 0–20 cm soil profile in a comparison between no-tillage at the fifth year of transition and conventional tillage (Carretta et al., 2021a). However, different dissipation dynamics between soil managements were likely biased by different inherent soil properties that masked some effects of tillage. Moreover, the water table depth was not monitored, which could have been an additional source of uncertainty with respect to soil management. Finally, some authors have suggested that the only recent conversion to conservation agriculture (< 5 years) does not result in a substantial change of physical and biochemical soil properties yet (Chakraborty et al., 2022; Piccoli et al., 2017). In such peculiar conditions, we hypothesized that the early adoption of CA could favor the mobility of GLP in soil, by offsetting the benefits that conservation practices may provide in relation to increased contaminant adsorption and degradation.

This work aimed to investigate in a set of eight lysimeters, i) the effect of conservation agriculture adoption during the transition period under different shallow water table conditions on GLP and AMPA dynamics and ii) the peculiar interactions of molecules with soil and water, influenced by their dissipation/formation processes, adsorption on soil particles, and transport to groundwater.

2. Materials and methods

2.1. Experimental site description

The experimental study was conducted between May and July 2019 at the Experimental Farm "L. Toniolo" of the University of Padova in Legnaro (45°21′ N; 11°57′ E, 8 m a.s.l.), northeastern Italy. The climate is sub-humid, with a mean annual temperature of 14.3 °C (9.7 and 19.3 °C as yearly min and max) and annual rainfall of about 870 mm, distributed uniformly throughout the year. The experimental site – originally set up in 1984 – consists of twenty drainable lysimeters of 1 m^2 area and 1.5 m depth. The bottom of each lysimeter is funnel-shaped and connected via an underground drain-pipe (1‰ slope) to an external tube equipped with a valve to regulate both the water table level and leaching discharge. Each lysimeter is filled with soil – Fluvi-Calcaric Cambisol (FAO-UNESCO, 2008), silty loam – excavated from the adjacent experimental farm, preserving the original soil horizons. A 20 cm thick of gravel was placed at the bottom of each lysimeter to facilitate water drainage and prevent soil washout. Each lysimeter is equipped with a unique automated monitoring system that serves a dual purpose: i) to monitor the soil water content and matric potential dynamics, with TDR (Time Domain Reflectometry) probes (CS635, Campbell Scientific Inc., Lincoln Nebraska, USA) and electronic tensiometers respectively (T4e, UMS GmbH, Munich, DE), both installed at 15, 30 and 60 cm depths; ii) to collect the pore-water at the same depths with polyethylene/nylon suction cups (SPE20, Meter Group, Munich, DE) with high solute concentration accuracy through automatic regulation of the suction equilibrium with the surrounding soil water tension. This is performed using continuous pore-water sampler vacuum regulation with the surrounding soil water tension, based on matric potential readings (Mencaroni et al., 2021; Morari, 2006). A system composed of a 5-Volt digital-analog conversion module (A04A, Campbell Scientific Inc., Lincoln Nebraska, USA) connected to an electronic vacuum regulator is employed by incorporating a pressure relief valve (ITV2091, SMC Corporation, Tokyo, J). The imposed negative pressure applied to pore-water samplers was in the range of − 2 to − 70 kPa. To control water fluxes and preserve the site from extreme weather events, an automated mobile roof was built over the whole area. The site is also equipped with a weather station (Decagon Devices Inc., Pullman, USA).

2.2. Lysimeter set-up and herbicide application

In the present study, eight lysimeters were used to evaluate the soil-water dynamic of GLP and AMPA under a combination of two shallow water table levels at 120 and 60 cm depth (hereafter called WT120 and WT60) and two crop management systems (conservation – CA – vs. conventional – CV – agriculture). The water table level was regulated manually every day (± 10 cm from the set reference level) by using a valve at the bottom of each lysimeter or by adding water manually, and a pressure switch was used to measure every 30 min the water level inside each lysimeter. The water table level was kept constant since 2011 (Longo et al., 2021a). No-tillage, cover crop cultivation, and crop rotation were the operations applied for conservation agriculture. On the contrary, conventional agriculture consisted of simulated harrowing operations performed at 25 cm depth by manual spading before seeding, incorporation of residues, and bare soil maintenance between growing seasons. The main crops were the same for CA and CV, maize (*Zea mays* L.) in 2018, and grain sorghum (*Sorghum bicolor* (L.) Moench) in 2019. In CA, rye (*Secale cereale* L.) was sown as a cover crop at a seed density of 130 kg ha^{-1} on November 5, 2018 (Fig. 1). The experimental design was a randomized block with two replicates (hereafter referred to as "a" and "b") for four treatments (CA60, CA120, CV60 and CV120). The commercial herbicide Pantox 360 SUPER™ (Arysta, Barclay chemicals R&D Ltd), containing 360 g l^{-1} of acid glyphosate, was applied in the eight lysimeters at a constant rate of 1.44 kg ha^{-1} using a manual sprayer at 2.5 bar pressure on May 10, 2019 (Fig. 1). Glyphosate was applied on

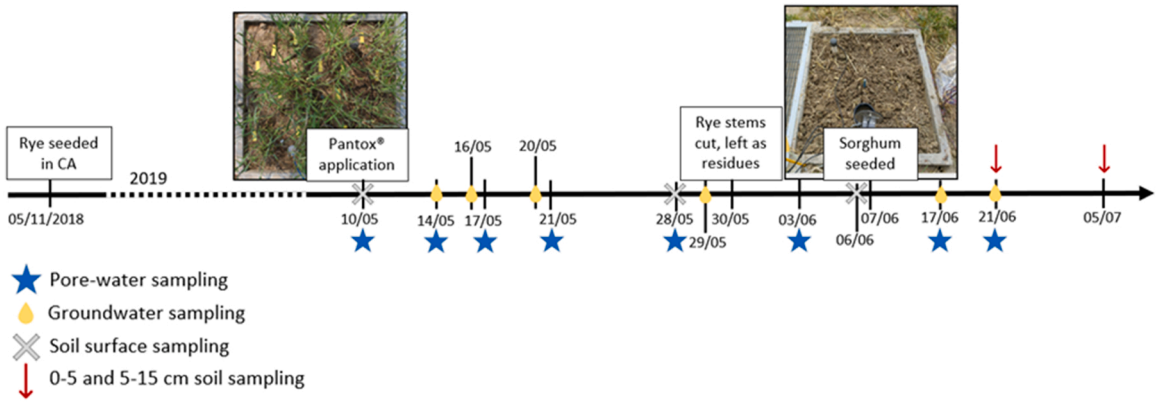

Fig. 1. Schematic representation of field set-up and water and soil sampling during the experiment. Picture of the Pantox application on rye refers to the replicas ("a" and "b") of CA treatment.

rye in CA and on bare soil in CV. Twenty days after the herbicide application, dry rye in CA was cut at the collar, shredded, and left on the soil surface as crop residues, while CV lysimeters were maintained bare during the whole experiment. The water input on each lysimeter was rainfall and irrigation (194.4 mm in 42 days). To note that GLP has not been used in the experimental plot since 2015.

2.3. Characterization of soil profiles

At the end of the experiment, disturbed soil samples were collected with a gouge auger (Ejjkelkamp Soil & Water, Giesbeek, NL) in each lysimeter along the soil profile at the corresponding depth of 0–20, 20–40, 55–70, and 95–110 cm, and later analyzed for chemical and physical properties. The auger had a 5 cm diameter to minimize soil disturbance. Samples were placed in plastic bags and later air-dried, homogenized, crushed with a mortar, and sieved at 2 mm. After sieving, samples were stored at room temperature in the dark until analysis. Soil texture was determined by using a particle size analyzer (Mastersizer 2000, Malvern Panalytical Ltd, Spectris Company, UK) according to the methodology described in Bittelli et al. (2019); soil organic carbon (SOC) and total nitrogen (total N) content were determined by flash combustion with a CNS-analyzer (vario MACRO cube, Elementar Analysensysteme GmbH, Langenselbold, D); pH and electrical conductivity (EC) were measured by an electrode in soil suspensions with soil to water ratio of 1:2.5 (w/v) and the cation exchange capacity (CEC) was determined using the $BaCl_2$-triethanolamine method (Table 1). Assimilable phosphorous (P Olsen) was also determined using the Olsen method, and iron (Fe) and aluminum (Al) oxides were analyzed in two forms: (i) poorly ordered Fe and Al oxides – hereafter labeled as Fe_{Ox} and Al_{Ox} – with the ammonium oxalate extraction in darkness method as (McKeague et al., 1971); (ii) SOM-chelated Fe and Al (hereafter labeled as Fe_{Som} and Al_{Som}), with the sodium pyrophosphate extraction method (pH = 10) (Bascomb, 1968). The determination of the extracts was performed by ICP-OES and the content was expressed as mg kg^{-1} (Table 2). The ratio between Al_{Som} and Fe_{Som} and SOM content (referred to as Al_{Som}/SOM and Fe_{Som}/SOM) was calculated by multiplying the SOC content by 1.72 to convert it to SOM. A high ratio means that, at equivalent SOM content, more Al and Fe are bound to SOM. A representative soil sample of WT60 and WT120 treatments was analyzed by X-ray powder diffraction (XRPD) to determine the soil mineral composition as in Piccoli et al. (2016). Analyses focused on the identification of the mineralogical phase in the bulk soil at different depths (Table 3). X-ray diffraction data were collected using a Panalytical X'Pert PRO MPD diffractometer equipped with a X'Celerator detector, a Co-anode X-ray tube and operating in Bragg-Brentano reflection geometry. Semiquantitative estimates of individual minerals were obtained by full profile analyses of diffraction data applying the Rietveld method as implemented in Topas v4.1 software.

2.4. Adsorption isotherms of glyphosate in the commercial product

Glyphosate sorption isotherms were determined by performing the batch adsorption experiment as reported by the OECD Guideline using the Batch Equilibrium Method (OECD, 2000). The commercial product Pantox 360 SUPER™ was used to better represent the herbicide sorption under field conditions. Five different concentrations of GLP in the range of 1–100 μg g^{-1} of dry soil were tested, with three replicates each. Adsorption isotherms were estimated for all lysimeters in different layers (0–20, 20–40, 55–70 and 95–110 cm) to represent the adsorption dynamic along the full soil profile. Uncontaminated soil, obtained from the sampling at the end of the experiment and checked for the lack of GLP and AMPA, was used for the adsorption experiment. Firstly, a solution of 0.01 M $CaCl_2$ was added to 1 g of the 2 mm-sieved and

Table 1
Average soil chemical and physical properties ± standard errors for CA and CV lysimeters. SOC is the soil organic carbon content (%), N is the total nitrogen (%), EC is the soil electrical conductivity (μS cm^{-1}), CEC is the cation exchange capacity (meq 100 g^{-1}), and Olsen P is the available phosphorous determined through the Olsen method (mg kg^{-1}).

Treatment	Depth	Particle size distribution %			pH	EC	SOC	N	Olsen P	CEC
	cm	Sand	Silt	Clay	-	μS cm^{-1}	%	%	mg kg^{-1}	meq 100 g^{-1}
CA	0–20	27.0 ± 1.3	56.1 ± 0.5	16.9 ± 0.9	7.8 ± 0.0	263.3 ± 6.6	0.96 ± 0.05	0.12 ± 0.01	47.3 ± 14.2	14.5 ± 0.5
	20–40	24.4 ± 2.1	57.2 ± 1.3	18.5 ± 0.9	8.2 ± 0.0	189.5 ± 6.8	0.69 ± 0.05	0.09 ± 0.01	21.8 ± 5.6	15.1 ± 0.4
	55–70	21.4 ± 2.0	58.8 ± 2.0	20.0 ± 0.1	8.3 ± 0.0	190.5 ± 3.1	0.57 ± 0.04	0.08 ± 0.01	11.2 ± 3.7	17.7 ± 0.8
	95–110	18.2 ± 0.6	61.1 ± 0.5	20.7 ± 0.2	8.2 ± 0.0	191.0 ± 3.1	0.58 ± 0.02	0.09 ± 0.01	14.9 ± 20.0	17.1 ± 0.3
CV	0–20	26.7 ± 0.5	56.9 ± 0.6	16.5 ± 0.3	7.8 ± 0.1	270.5 ± 20.9	0.88 ± 0.04	0.12 ± 0.00	41.2 ± 10.7	13.9 ± 0.1
	20–40	26.7 ± 0.5	56.4 ± 0.1	17.0 ± 0.5	8.2 ± 0.1	194.1 ± 14.4	0.73 ± 0.02	0.10 ± 0.00	21.7 ± 7.1	14.3 ± 0.0
	55–70	17.9 ± 2.7	61.2 ± 2.1	20.9 ± 0.6	8.3 ± 0.0	197.5 ± 9.8	0.60 ± 0.01	0.09 ± 0.00	11.9 ± 3.5	18.2 ± 0.5
	95–110	18.5 ± 0.5	58.8 ± 1.9	20.2 ± 0.7	8.3 ± 0.0	188.0 ± 6.8	0.64 ± 0.02	0.09 ± 0.00	20.1 ± 4.3	17.2 ± 0.7

Table 2
Al and Fe characterization of soil profiles as averaged between replicates. Fe_{Ox} and Al_{Ox} (mg kg^{-1}) are poorly-ordered oxides, Fe_{Som} and Al_{Som} (mg kg^{-1}) are SOM-chelated Fe and Al, Fe_{Som}/SOM and Al_{Som}/SOM (%) are the ratio with SOM. The significance was tested for depths and treatments: values followed by the same letter are not statistically different at $p > 0.05$.

Treatment	Depth	Fe_{Ox}	Al_{Ox}	Fe_{Som}	Al_{Som}	Fe_{Som}/SOM	Al_{Som}/SOM
	cm	mg kg^{-1}	mg kg^{-1}	mg kg^{-1}	mg kg^{-1}	%	%
CA60	0–20	1530 ± 46	554 ± 25	260 ± 29	173 ± 16	1.6 ± 0.2	1.0 ± 0.1
	20–40	1620 ± 73	583 ± 30	202 ± 37	150 ± 29	1.6 ± 0.2	1.2 ± 0.2
	55–70	1920 ± 4	649 ± 5	205 ± 38	167 ± 29	2.0 ± 0.3	1.6 ± 0.2
	95–110	2180 ± 128	671 ± 16	215 ± 44	179 ± 37	2.1 ± 0.4	1.7 ± 0.3
CA120	0–20	1840 ± 48	591 ± 17	335 ± 21	231 ± 2	2.1 ± 0.4	1.4 ± 0.2
	20–40	2010 ± 154	645 ± 81	347 ± 10	276 ± 10	3.2 ± 0.6	2.5 ± 0.5
	55–70	2220 ± 272	724 ± 84	388 ± 14	328 ± 13	4.3 ± 0.8	3.7 ± 0.7
	95–110	2070 ± 269	692 ± 74	389 ± 2	325 ± 7	4.2 ± 0.3	3.5 ± 0.2
CV60	0–20	1780 ± 94	573 ± 0	283 ± 16	203 ± 15	2.0 ± 0.0	1.4 ± 0.0
	20–40	1910 ± 290	609 ± 55	313 ± 26	237 ± 24	2.5 ± 0.1	1.9 ± 0.1
	55–70	2000 ± 81	672 ± 1	366 ± 30	297 ± 35	3.5 ± 0.2	2.9 ± 0.3
	95–110	2090 ± 137	706 ± 48	374 ± 40	296 ± 48	3.5 ± 0.2	2.7 ± 0.3
CV120	0–20	1740 ± 203	574 ± 52	289 ± 30	208 ± 30	1.8 ± 0.1	1.3 ± 0.1
	20–40	1660 ± 41	583 ± 6	294 ± 43	228 ± 36	2.3 ± 0.2	1.8 ± 0.2
	55–70	1790 ± 391	603 ± 110	344 ± 61	275 ± 58	3.4 ± 0.6	2.7 ± 0.6
	95–110	1810 ± 93	585 ± 52	398 ± 26	289 ± 47	3.6 ± 0.3	2.6 ± 0.4
Depth	0–20	1720 ± 63 *b*	573 ± 12 *b*	291 ± 14	204 ± 11 *b*	1.9 ± 0.1 *b*	1.3 ± 0.1 *b*
	20–40	1800 ± 9 *ab*	605 ± 22 *ab*	289 ± 24	223 ± 20 *ab*	2.4 ± 0.2 *b*	1.9 ± 0.2 *b*
	55–70	1980 ± 109 *ab*	662 ± 31 *a*	326 ± 31	267 ± 27 *a*	3.3 ± 0.4 *a*	2.7 ± 0.3 *a*
	95–110	2040 ± 82 *a*	663 ± 26 *a*	344 ± 31	272 ± 25 *a*	3.3 ± 0.3 *a*	2.7 ± 0.3 *a*
Treatment	CA60	1810 ± 102	614 ± 20	220 ± 17 *b*	167 ± 12 *b*	1.8 ± 0.1 *b*	1.4 ± 0.1 *c*
	CA120	2040 ± 94	663 ± 32	365 ± 10 *a*	290 ± 15 *a*	3.5 ± 0.4 *a*	2.8 ± 0.4 *a*
	CV60	1950 ± 78	640 ± 24	334 ± 18 *a*	259 ± 20 *a*	2.9 ± 0.3 *a*	2.2 ± 0.2 *a*
	CV120	1750 ± 88	586 ± 25	331 ± 23 *a*	250 ± 21 *a*	2.8 ± 0.3 *a*	2.1 ± 0.3 *b*

Table 3
Mineralogical composition of soil (weight %) averaged among treatments ± standard errors divided by layers, determined from XRPD.

	0–20 cm	**20–40 cm**	**55–70 cm**	**95–110 cm**
	weight %			
Dolomite	26.0 ± 0.0	26.5 ± 0.5	27.0 ± 0.0	26.0 ± 0.0
Quartz	24.5 ± 0.5	26.0 ± 1.0	23.0 ± 0.0	24.5 ± 0.5
Muscovite	21.0 ± 0.0	19.5 ± 0.5	20.0 ± 0.0	20.5 ± 0.5
Feldspar	15.0 ± 0.0	13.5 ± 0.5	14.0 ± 0.0	12.5 ± 0.5
Calcite	7.0 ± 0.0	7.5 ± 0.5	8.0 ± 0.0	8.5 ± 0.5
Chlorite-like	7.0 ± 0.0	7.5 ± 0.5	7.0 ± 0.0	7.5 ± 0.5

air-dried soil in 50-ml polypropylene tubes with a corresponding ratio of 1:40 and then shaken at 200 rpm for 24 h at 20 °C. Then, the soil slurry was spiked with the corresponding Pantox® solution and shaken for 24 h. The tubes were centrifuged (6000 rpm for 20 min) and an aliquot of the supernatant was filtered using a regenerated cellulose membrane filter (pore size 0.20 μm) and stored in the fridge at + 4 °C before UHPLC-MS analysis. Samples were derivatized as reported in Carretta et al. (2019).

Adsorption data were fitted by nonlinear regression to the Freundlich adsorption isotherm model:

$$C_s = K_f C_w^{\left(\frac{1}{n}\right)} \quad (1)$$

where C_s (μg g^{-1}) is the adsorbed amount, C_w (μg ml^{-1}) is the concentration in the aqueous phase, K_f [$\mu g^{1-1/n}$ $(ml)^{1/n}$ g^{-1}] is the Freundlich adsorption coefficient and 1/n is a measure of adsorption intensity and nonlinearity. Small 1/n values indicate the saturation of soil at high GLP contents.

2.5. Water sample collection and quantification of GLP and AMPA

Pore-water samples were collected with suction cups at 15, 30 and 60 cm depth for a total of seven non-consecutive days, starting on May 14 until June 21. Pore-water samples were collected in 1000 ml high-density polyethylene bottles (Nalgene™, Thermo Scientific, Waltham, Massachusetts, USA), transported to the laboratory where they were stored in a refrigerator (+4 °C), and then analyzed by UHPLC-MS for GLP and AMPA concentration using the procedure reported by Carretta et al. (2019) (recovery percentages, limit of detection – LOD – and limit of quantification – LOQ – were 88%, 0.2, and 0.5 μg l^{-1}, respectively for GLP; 89%, 0.05 and 0.1 μg l^{-1} respectively for AMPA). The concentration of contaminants out of the calibration range (0.2–100 μg l^{-1} for GLP and 0.05–100 μg l^{-1} for AMPA) was appropriately diluted. Before the herbicide application, pore-water was sampled in all lysimeters at each depth to measure GLP and AMPA background concentration, which resulted < LOQ. Groundwater was collected at the bottom valve of each lysimeter when the water table was 10 cm above the set level, after rainfall or irrigation, and managed in the same way as reported for pore-water. Water runoff events did not occur throughout the experiment.

2.6. Soil sample collection and quantification of GLP and AMPA

Soil samples were collected starting on the day of the herbicide application and then after 18 and 27 days. Sampling was performed on two randomly selected points within each lysimeter at 1 cm depth (hereafter referred to as *surface soil*) and then bulked. To note that, for CA, the sample included residues left in the field from the previous crop. Two additional samplings, on June 21 and July 7 (day 42 and 56 after GLP application, respectively), were performed at two depths (0–5 and 5–15 cm) at each lysimeter to determine the residual amount of GLP and AMPA. Once collected in plastic bags, soils were transported to the laboratory. Samples were air-dried (20 °C) and sieved at 2 mm before analysis. The extraction procedure to analyze the concentration of GLP and AMPA in soil samples was performed as reported in Mencaroni et al. (2022). Then the samples were analyzed by HPLC-MS. The LOD and LOQ were 15 and 50 μg kg^{-1} for GLP, and 6 and 20 μg kg^{-1} for AMPA. Percentage recoveries were 91–115% for GLP and 83–98% for AMPA. The concentration of contaminants out of the calibration range (1.23–123 μg l^{-1} for GLP and 0.49–123 μg l^{-1} for AMPA) was appropriately diluted. Soil samples before the herbicide application were also

collected and analyzed for the background concentration, resulting to be < LOQ.

2.7. Data analysis

Adsorption coefficients (K_f and 1/n) were calculated using the Solver tool in Excel MS Office, minimizing the sum of squared error. Pearson correlation coefficients between K_f and soil properties (N = 32) were tested at two significance levels (p = 0.05 and p = 0.01), and a three-way ANOVA with a Tukey post-hoc test was performed to test significant differences in K_f and soil properties between soil managements (CA and CV), WT level (120 and 60) and soil depths (0–20, 20–40, 55–70 and 95–110 cm). A Kruskal-Wallis non-parametric test was performed to test the significance ($p < 0.05$) between treatments on GLP concentration in groundwater. When GLP concentration was below the LOQ (censored data were >50%), the value was set as one-half the LOQ to estimate the summary statistics, as reported by Gilbert (1988). Statistical analyses were performed using R (R Core Team, 2017).

3. Results

3.1. Soil properties

Soil properties showed a differentiation among soil layers (Tables 1 and 2). Silt was the predominant texture fraction which slightly increased with depth, from 56% in 0–20 cm to about 60% in the deepest layers (> 55 cm). A similar trend was observed for clay, which ranged from 17% to 20% with no relevant differences between CA and CV. Profile stratification was also reflected in the chemical properties, showing contrasting values of pH (7.8 vs. 8.2), SOC (0.9 vs. 0.6%) and P Olsen (> 40 vs. 17 mg kg^{-1}) between the top layer and the deepest ones. Some slight increase of SOC content was found in 0–20 cm in CA (0.97 ± 0.05%) than CV (0.88 ± 0.04%). Cation exchange capacity (CEC) increased with depth, reaching a maximum of 18 meq 100 g^{-1} in 55–70 cm, being more affected by clay than SOC content. Fe_{Ox} and Al_{Ox} – as well as Fe_{Som} and Al_{Som} – were also found to increase with depth, from an average of 1721 ± 63 and 573 ± 12 mg kg^{-1} in 0–20 cm to 2038 ± 82 and 663 ± 27 mg kg^{-1} in 95–110 cm respectively (Table 2). The ratio between Fe and Al with SOM almost doubled with depth due to their opposite trends within the soil profile. The mineralogical composition of the soil was similar among layers (Table 3), highlighting the predominance of layered silicates (~66%) – of which 42% were aluminosilicates (muscovite and chlorite-like fraction) – in the carbonate phase (dolomite and calcite, 34%).

3.2. GLP adsorption isotherms

The Freundlich equation described with good accuracy the soil-water GLP repartition (Table 4, $R^2 \geq 0.90$) for all depths and in the different management systems (Fig. 2). The 1/n parameter was always < 1, suggesting that non-linear adsorption occurred in all cases. Some 1/n reduction was found at increasing depth of investigation, which revealed the skewness of the curve was enhanced along the soil profile. To note that at 55–70 cm layer, 1/n reached the lowest average value (0.39 ± 0.00), and then increased again (0.60 ± 0.06 at 95–110 cm) regardless the groundwater and cultivation management. On the contrary, K_f has always increased with soil depth, highlighting that GLP-soil particle interaction was enhanced from 0 to 20 cm (27.5 ± 2.0) to 20–40 cm (46.5 ± 2.1), 55–70 cm (56.0 ± 2.7) and 95–110 cm (74.0 ± 3.7). Several soil properties significantly affected GLP adsorption (Table 5), positively like clay and CEC (r = 0.75 and 0.62), and negatively like Olsen P, SOC content and EC (r = −0.57, −0.69 and −0.67 respectively). Furthermore, SOM-chelated Al and Fe – reported as Al_{Som}/SOM and Fe_{Som}/SOM – slightly influenced GLP adsorption, having r = 0.37 in both ($p < 0.05$).

Table 4
Freundlich adsorption coefficients averaged between replicates (K_f and 1/n) for GLP for different treatments and different soil depths ± standard errors. The significance is reported for depths and treatments: values followed by the same letter are not statistically different at $p > 0.05$.

Treatment	Depth	K_f	1/n	R^2
CA60	0–20	27.2 ± 6.2	0.78 ± 0.16	0.91
	20–40	52.3 ± 1.6	0.86 ± 0.01	0.99
	55–70	66.4 ± 1.2	0.48 ± 0.00	0.96
	95–110	78.0 ± 1.6	0.58 ± 0.05	0.98
CA120	0–20	32.2 ± 0.5	0.86 ± 0.15	0.99
	20–40	44.4 ± 2.1	0.59 ± 0.04	0.94
	55–70	49.0 ± 2.7	0.39 ± 0.00	0.92
	95–110	62.6 ± 1.0	0.46 ± 0.01	0.98
CV60	0–20	21.3 ± 0.1	0.70 ± 0.03	0.97
	20–40	38.9 ± 0.1	0.50 ± 0.01	0.91
	55–70	54.3 ± 2.3	0.49 ± 0.04	0.90
	95–110	78.2 ± 0.5	0.56 ± 0.04	0.97
CV120	0–20	28.9 ± 3.3	0.75 ± 0.02	0.96
	20–40	50.4 ± 0.0	0.87 ± 0.06	0.92
	55–70	54.2 ± 4.4	0.49 ± 0.01	0.94
	95–110	77.0 ± 14.3	0.60 ± 0.06	0.95
Depth	0–20	27.5 ± 2.0 *c*	0.77 ± 0.05 *a*	
	20–40	46.5 ± 2.1 *b*	0.70 ± 0.06 *a*	
	55–70	56.0 ± 2.7 *b*	0.46 ± 0.02 *b*	
	95–110	74.0 ± 3.7 *a*	0.55 ± 0.03 *b*	
Treatment	CA60	56.0 ± 7.3	0.68 ± 0.07	
	CA120	47.1 ± 4.1	0.57 ± 0.07	
	CV60	48.2 ± 7.9	0.56 ± 0.03	
	CV120	52.6 ± 7.1	0.68 ± 0.06	

3.3. GLP and AMPA concentration in soil

At the soil surface (0–1 cm), GLP was found at very high concentrations (Table 6), ranging from 9170 to 13,500 μg kg^{-1} a few hours after the application (day 0, hereafter referred to C_0). After 18 days, GLP sharply decreased compared to the initial concentration (from −88.3% to a maximum of −97.2%), ending to an almost complete dissipation on day 27, when GLP was less than 1.5% of C_0. Generally, CA showed a lower amount of GLP at day 0 (11,700 ± 1060 μg kg^{-1}) than CV (13,000 ± 353 μg kg^{-1}), due to the presence of rye which intercepted part of the herbicide spray. As for the parent molecule, AMPA was already detected few hours after the application with a significant difference between treatments, being the average concentration of 833 ± 142 and 1950 ± 70 μg kg^{-1} in CA and CV, respectively. A similar difference was found on day 18 when the average AMPA concentration was 537 ± 15 in CA and 1270 ± 84 μg kg^{-1} in CV. At day 18, the AMPA reduction was 48% in CA60 and 12% in CA120, highlighting different rates of transformation/dissipation according to WT. After 27 days, AMPA in CA was reduced to 190 ± 37 and in CV to 415 ± 56 μg kg^{-1}. A different dynamic between crop managements was found at 0–5 and 5–15 cm depth (Table 7). In fact, GLP was always < LOQ in CA in both layers, suggesting that a full dissipation already occurred at day 42. In CV, GLP was found in 2 out of 4 times in both sampling days 42 and 56 at 0–5 cm depth, mostly with a shallower water table. Conversely, AMPA was detected in CA in 3 out of 4 samples (42 days, 81.1 ± 5.6 μg kg^{-1}) at 0–5 cm, and down to 15 cm only in one lysimeter at 56 days. In CV, the metabolite was always detected on both layers (157 ± 45 and 90.5 ± 17 μg kg^{-1} at 0–5 and 5–15 cm respectively at 42 days), except for CV120a where AMPA was < LOQ at 0–5 cm on day 56.

3.4. GLP and AMPA dynamic in soil pore-water

A total of 142 pore-water samples were collected and analyzed for GLP and AMPA content. GLP was > LOQ in 53% of CA samples with deep water table level (120 cm), a frequency that increased to 81% in CV60. The maximum peak of GLP was reached after 4 days at 15 cm depth (Fig. 3), with the highest detected in CV120a (131 μg l^{-1}) and the

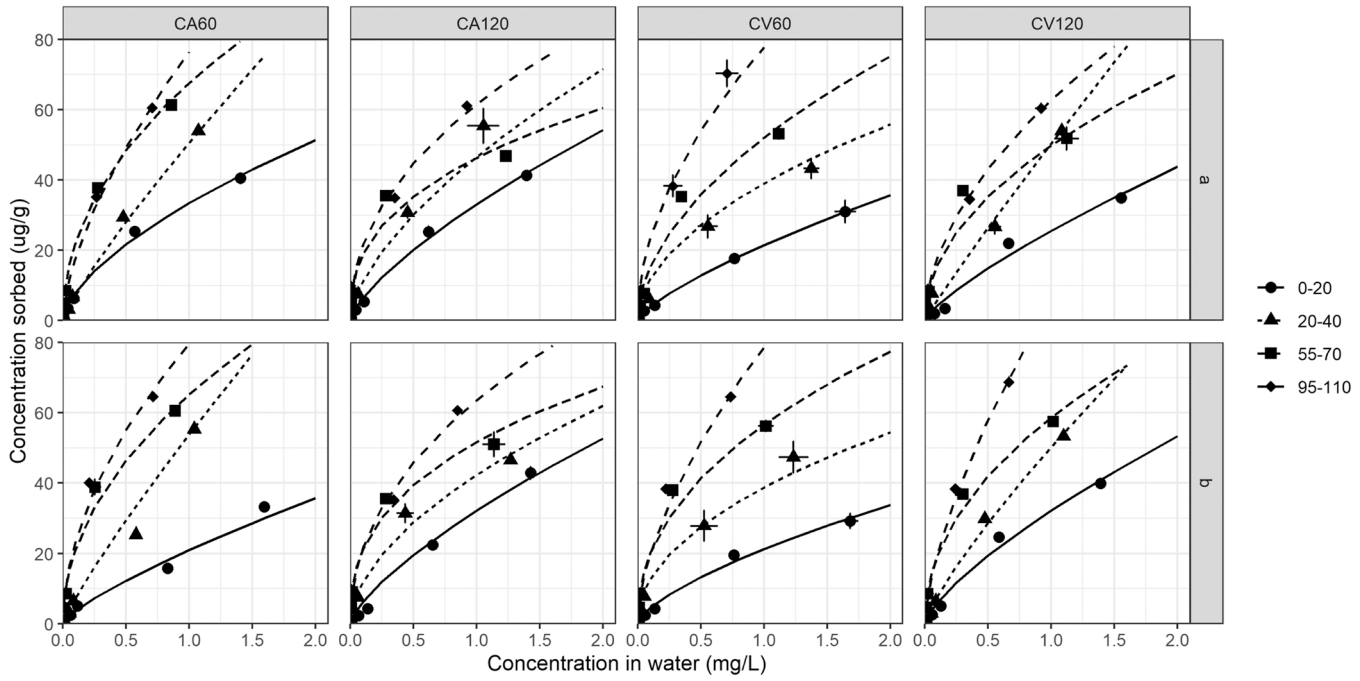

Fig. 2. Freundlich adsorption isotherms of GLP at different depths in the four treatments and two replicates ("a" and "b"). Symbols are observed values reported as the mean ± standard error and lines represent the fitting curves.

Table 5
Pearson's correlation coefficients (r) between estimated Freundlich adsorption coefficients (K_f and 1/n) for GLP and selected soil properties (N = 32). Values with ** indicate that the correlation is significant at 0.01 level and * at 0.05.

	Sand	Silt	Clay	SOC	pH	EC	CEC	Olsen P	Al_{Ox}	Fe_{Ox}	Al_{Som}/SOM	Fe_{Som}/SOM	K_f
Sand													
Silt	-0.95 **												
Clay	-0.89 **	0.71 **											
SOC	0.58 **	-0.46 **	-0.66 **										
pH	-0.55 **	0.44 *	0.62 **	-0.85 **									
EC	0.44 *	-0.33	-0.52 **	0.72 **	-0.90 **								
CEC	-0.74 **	0.60 **	0.80 **	-0.70 **	0.67 **	-0.55 **							
P Olsen	0.61 **	-0.49 **	-0.68 **	0.86 **	-0.87 **	0.74 **	-0.72 **						
Al_{Ox}	-0.28	0.20	0.35	-0.58 **	0.47 **	-0.36 *	0.42 *	-0.54 **					
Fe_{Ox}	-0.25	0.21	0.26	-0.50 **	0.43 *	-0.37 *	0.34	-0.44 *	0.92 **				
Al_{Som}/SOM	-0.48 **	0.43 *	0.46 **	-0.72 **	0.67 **	-0.50 **	0.64 **	-0.64 **	0.73 **	0.66 **			
Fe_{Som}/SOM	-0.46 **	0.43 *	0.43 *	-0.70 **	0.65 **	-0.47 **	0.62 **	-0.58 **	0.67 **	0.61 **	0.99 **		
K_f	-0.67 **	0.53 **	0.75 **	-0.69 **	0.69 **	-0.67 **	0.62 **	-0.57 **	0.31	0.30	0.37 *	0.37 *	
1/n	0.58 **	-0.51 **	-0.51 **	0.71 **	-0.59 **	0.41 *	-0.71 **	0.73 **	-0.48 **	-0.52 **	-0.67 **	-0.65 **	-0.41 *

lowest in CA60b (42.3 μg l^{-1}). On the same day, GLP was found at 60 cm depth at concentrations ranging from 20.5 to 94.1 μg l^{-1} (in CA60a and CV60b respectively). In some cases, the maximum peak at 30 and 60 cm depth was delayed at day 7 instead of 4. After 7 days, GLP concentration started to decrease mostly at 15 cm and after 11 days, it was sharply reduced to an average value of 4.1 ± 1.9 μg l^{-1}. In intermediate and deepest layers, GPL was only occasionally detected. Some lysimeters showed a delayed increment, like CA60a at 15 cm (day 38, 33.1 μg l^{-1}) and CV60b at 30 cm depth (day 24, 54.2 μg l^{-1}). Moreover, at WT60 and 60 cm sampling depth, GLP reached an average of 6.9 ± 0.2 μg l^{-1} after 20 days, which only slightly changed until the end of the experiment (Fig. 3). In general, CV lysimeters showed higher GLP concentration at 15 cm – 18.9 ± 8.0 and 30.3 ± 13.3 μg l^{-1} for CV60 and CV120 respectively – then decreasing at 30 and 60 cm.

Contrary to GLP, AMPA was detected only in 5% of CA, regardless the water table level, 14% of samples in CV60 and 32% in CV120. It was only found at 15 cm, starting from day 4 until 24 after the application (Fig. 4), while at 60 cm it was only detected in CV120a after 7 days (2.7 μg l^{-1}).

3.5. GLP and AMPA in the groundwater

During the experiment, groundwater was monitored from May 14 (day 4) to June 27 (day 48) for a total of 44 analyses. The GLP detection frequency was higher in CV than CA (Fig. 5). On day 4, GLP was firstly detected in all lysimeters after 30 mm of rainfall, at an average concentration of 7.2 ± 0.1 μg l^{-1}. On day 6, GLP was found in WT120, ranging from 7.5 to 22.1 μg l^{-1}, while it was < LOQ in WT60 (except for CV60b). After a cumulative rainfall of 51 mm (i.e. 17–18 days from the herbicide application), GLP was detected again in all lysimeters at concentrations of 6.90 ± 0.30 μg l^{-1}. The concentration was < LOQ in almost all cases after 38 days, while at day 48 GLP only occurred in CV (2 out of 4 lysimeters). All along the experimentation, GLP median concentrations were lower in CA (WT60 and WT120 were 0.30 ± 1.10 and 3.40 ± 2.40 μg l^{-1}) than CV (WT60 and WT120 were 6.6 ± 1.5 and 7.0 ± 1.50 μg l^{-1}), but the high variability made differences not statistically significant $p < 0.05$ (Fig. 6). Contrary to GLP, AMPA was always < LOQ in the groundwater.

Table 6
GLP and AMPA concentration in the soil surface (0–1 cm layer) at increasing day intervals in the eight lysimeters ("a" and "b" represent the two replicas). Day 0 refers to the day of herbicide distribution (May 10, 2019). The percentage of GLP dissipated and the formation of AMPA (GLP_{Diss} and $AMPA_{Formed}$) are also reported.

		GLP	AMPA	GLP_{Diss}	$AMPA_{Formed}$
Treatment	Day	μg kg^{-1}	μg kg^{-1}	%	%
CA60 a	0	13,500	1120		11.2
	18	472	579	96.5	5.8
	27	113	234	99.2	2.3
CA60 b	0	13,400	1020		10.3
	18	377	537	97.2	5.4
	27	70	91	99.5	0.9
CA120 a	0	9170	657		9.8
	18	681	516	92.6	7.7
	27	87	179	99.1	2.7
CA120 b	0	10,700	531		7.0
	18	811	517	92.4	6.8
	27	87	257	99.2	3.4
CV60 a	0	12,000	1810		18.6
	18	779	1040	93.5	10.7
	27	153	412	98.7	4.2
CV60 b	0	13,500	1880		17.4
	18	1580	1450	88.3	13.4
	27	254	499	98.1	4.6
CV120 a	0	12,900	1970		18.8
	18	782	1280	93.9	12.2
	27	149	491	98.8	4.7
CV120 b	0	13,500	2140		19.3
	18	1100	1300	91.9	11.8
	27	105	259	99.2	2.3

Table 7
GLP and AMPA concentration in soil at 0–5 and 5–15 cm at 42 and 56 days after application in the eight lysimeters ("a" and "b" represent the two replicas). When the molecule concentration was below the limit of quantification, "<LOQ" is reported in the Table.

		GLP		AMPA	
Treatment	Day	0–5 cm	5–15 cm	0–5 cm	5–15 cm
		μg kg^{-1}	μg kg^{-1}	μg kg^{-1}	μg kg^{-1}
CA60 a	42	< LOQ	< LOQ	72.2	< LOQ
	56	< LOQ	< LOQ	68.0	< LOQ
CA60 b	42	< LOQ	< LOQ	< LOQ	< LOQ
	56	< LOQ	< LOQ	< LOQ	< LOQ
CA120 a	42	< LOQ	< LOQ	91.5	< LOQ
	56	< LOQ	< LOQ	< LOQ	< LOQ
CA120 b	42	< LOQ	< LOQ	79.7	< LOQ
	56	< LOQ	< LOQ	< LOQ	78.7
CV60 a	42	98.3	< LOQ	240	140
	56	86.3	48.7	214	94.8
CV60 b	42	< LOQ	< LOQ	72.2	78.0
	56	52.6	48.7	171	101
CV120 a	42	69.3	< LOQ	232	68.0
	56	< LOQ	< LOQ	< LOQ	138
CV120 b	42	< LOQ	< LOQ	85.8	76.0
	56	< LOQ	< LOQ	81.9	90.4

4. Discussion

4.1. Adsorption of GLP and AMPA to soil particles

Results about GLP adsorption isotherms indicated that most of the variability was observed with depth, regardless the management practices. The adsorption coefficient (K_f) resulted approximately three times greater in the deepest layer than in the surface layer, and 1/n decreased at increasing depth. Despite such variability, it was generally observed a low affinity for the soil phase of the Cambisol under investigation, with K_f that never exceeded 80, which is a relatively low coefficient compared to other studies (Candela et al., 2007; Piccolo et al., 1994; Okada et al., 2016). This might be explained by the alkaline reaction of the soil under investigation, which has maximized the negative electrical charges of GLP at high pH, thus limiting its adsorption to soil particles due to its polyprotic nature (De Gerónimo and Aparicio, 2021; Borggaard and Gimsing, 2008). Similar values were found by Accinelli et al. (2005), which performed an adsorption study on a surface soil layer (0–20 cm) having pH = 8.1 and clay content similar to ours (14%), resulting in a K_f of 43. Conversely, other authors reported higher adsorption than ours (K_f = 166) at lower pH (6.1) and similar clay content (17%) (Autio et al., 2004). Noteworthy is also the work of Carretta et al. (2021a), which analyzed GLP adsorption in the same soil as in the present study, but only in the surface layer. The authors compared the effect of conventional and no-tillage practices on GLP adsorption, highlighting a K_f that was statistically lower in the first than in the second treatment (around 28 and 51, respectively) in the 0–20 cm profile. In our study, the surface layer K_f was on average 27.5 ± 2 and did not statistically differ between treatments (Table 6). The missing difference between agricultural management can be due to the recent conversion of the soil to CA practices (about 2 years) which might have masked the potential effect of CA on the adsorption dynamic of GLP, e.g., due to an increase in SOC (Page et al., 2020; Patle et al., 2013) which might favor the formation of poorly-order Fe and Al oxides (Borggaard and Gimsing, 2008). In the present work, the slight difference in soil properties between CA and CV, did not modify K_f between managements. Similarly, the WT management did not affect significantly the GLP adsorption, suggesting that a prolonged change in soil moisture condition was not a driver able to modify the physicochemical soil properties that could affect it.

Multiple soil properties contributed to the adsorption dynamic of GLP in the studied soil (Table 5), as emphasized by the positive correlation of K_f with both clay and CEC, and the negative one with phosphorus (Olsen P) that emphasized the strong competition for the same sorption sites (De Jonge et al., 2001; Gimsing and Borggaard, 2002; Munira et al., 2016). This phenomenon is particularly relevant in intensive agricultural systems such as those of the low-lying Venetian plain, where progressive saturation of soil sorption capacities can occur due to continuous application of P-rich mineral and organic fertilizers (Pizzeghello et al., 2011), enhancing the risk of GLP mobility to groundwater. This was also corroborated by the positive correlation that was found between 1/n and Olsen P (Table 7), which suggests a low rate of GLP sorption (1/n closer to 1) onto soil particles as the competition with P increased. The SOC content, like EC, seemed to have a negative influence on K_f: In this case, the effect of repulsive negative charges of SOM might have blocked available sorption sites for GLP, reducing its adsorption (Borggaard and Gimsing, 2008). No significant relationships were found between K_f and Al_{Ox} or Fe_{Ox}, despite GLP is in general highly adsorbed onto variable-charged surfaces, like Al and Fe oxides. For example, significant correlations were found by Sidoli et al. (2016) between K_f and Al_{Ox}, although the greater variability of their analyzed soils compared to ours (e.g., pH was in the range 6.1–8.0, Al_{Ox} was in the range 1200–2200 mg kg^{-1}) may have contributed to increasing the linear interdependence between adsorption and mineralogy. On the contrary, SOM-chelated Al and Fe, which are metals complexed with humic substances, have likely acted as metal bridges (Gerke, 2010), influencing GLP sorption in a limited way, due to the increasing Al and Fe amount at equal SOM along with the soil profile (Table 2), as also found in other northern soils of the Veneto region (Mencaroni et al., 2022). A strong correlation was found between 1/n and Al and Fe bound to SOM, as with poorly-ordered Al and Fe oxides, suggesting that at high Al and Fe content the non-linearity of the curve increased, thus reflecting a tendency to decrease the sorption at increasing GLP concentrations in solution. Worth of note was also the slight change in the soil mineralogy found at different soil depths (Table 3), such as the calcite that was found to increase along the soil profile. Some authors reported that anionic pesticides are slightly adsorbed by calcite (Clausen et al., 2001), indicating that this fraction cannot play a major role in pesticides adsorption as compared with clay and oxide minerals (e.g.

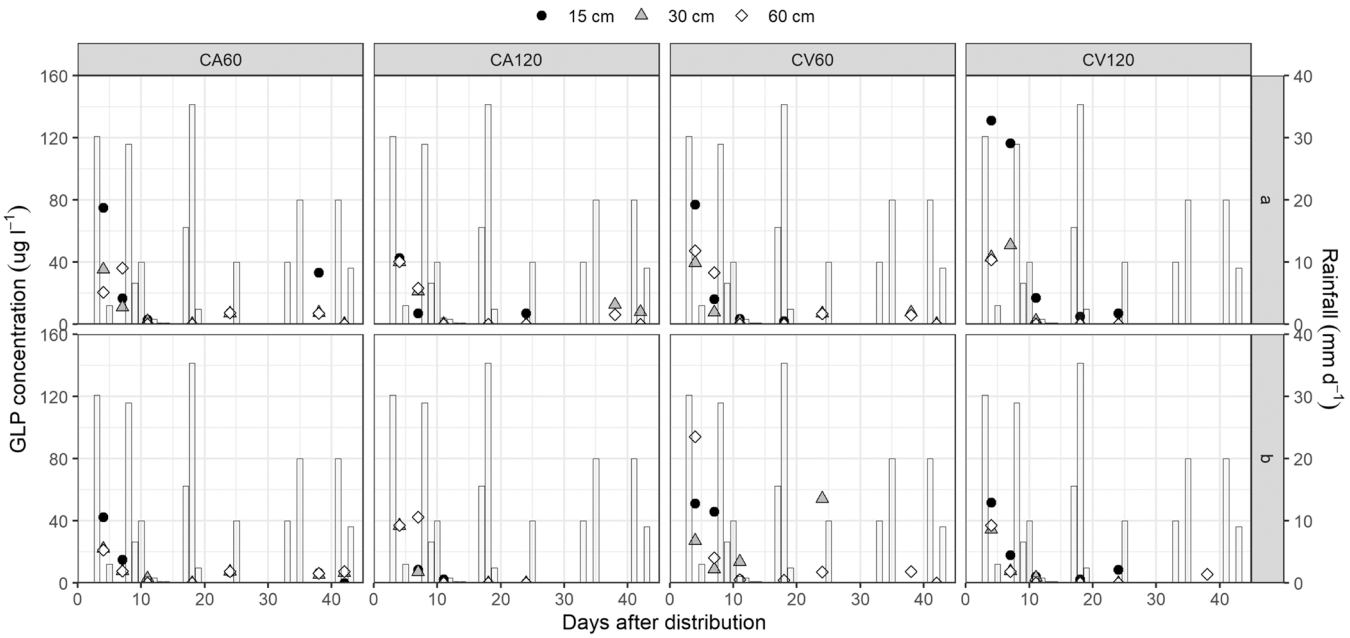

Fig. 3. GLP concentration in soil pore-water at the three different depths (15 cm - black circle, 30 cm - grey triangle, 60 cm - white rhombus) for the eight studied lysimeters ("a" and "b" represent the two replicas). Bars refer to simulated rainfall amount (mm) during the sampling period.

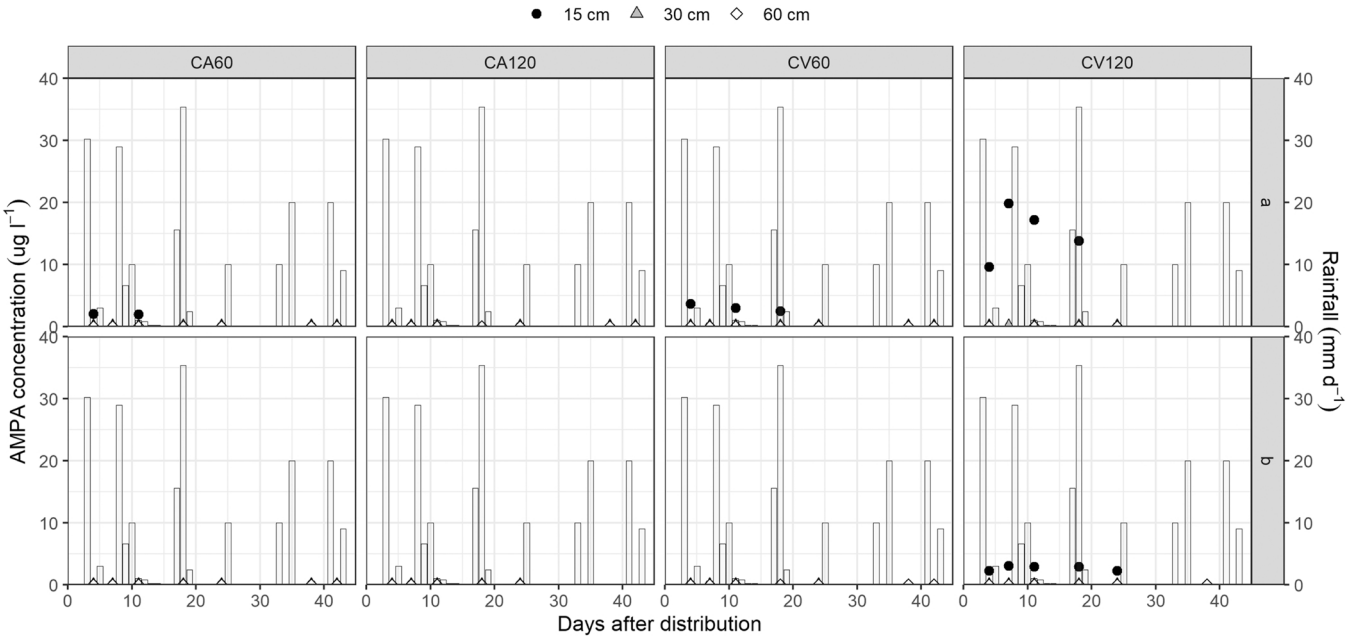

Fig. 4. AMPA concentration in soil pore-water at the three different depths (15 cm - black circle, 30 cm - grey triangle, 60 cm - white rhombus) for the eight studied lysimeters ("a" and "b" represent the two replicas). Bars refer to simulated rainfall amount (mm) during the sampling period.

gibbsite or ferrihydrite), but may emphasize it. In addition, the mineralogical composition of the soil was characterized by the predominance of silicate minerals. Although layered silicates have only few permanent and negatively charged adsorption sites (OH groups) in the octahedral layer (Borggaard and Gimsing, 2008) and are a limited source of exchangeable cations in soils due to the low CEC (Kumari and Mohan, 2021), it can be hypothesized a complexation of GLP by cations released from clay silicates via a cation-exchange reaction with solution protons, as reported by Glass (1987).

4.2. Mobility and occurrence of GLP and AMPA along the soil profile

Glyphosate in water was detected soon after its application at all depths and in groundwater, regardless of agricultural and WT management, emphasizing the likely occurrence of bypass flow and reduced GLP adsorption when rainfall time was close to its application (Jarvis, 2007), enhancing the leaching potential of the molecule to the groundwater (Székács et al., 2015; Pazikowska-Sapota et al., 2020). Despite the Cambisol under investigation being poorly structured, previous research that combined modeling and X-ray μCT analysis demonstrated that shallow water table conditions can enhance solute movement through non-equilibrium preferential pathways (Mencaroni

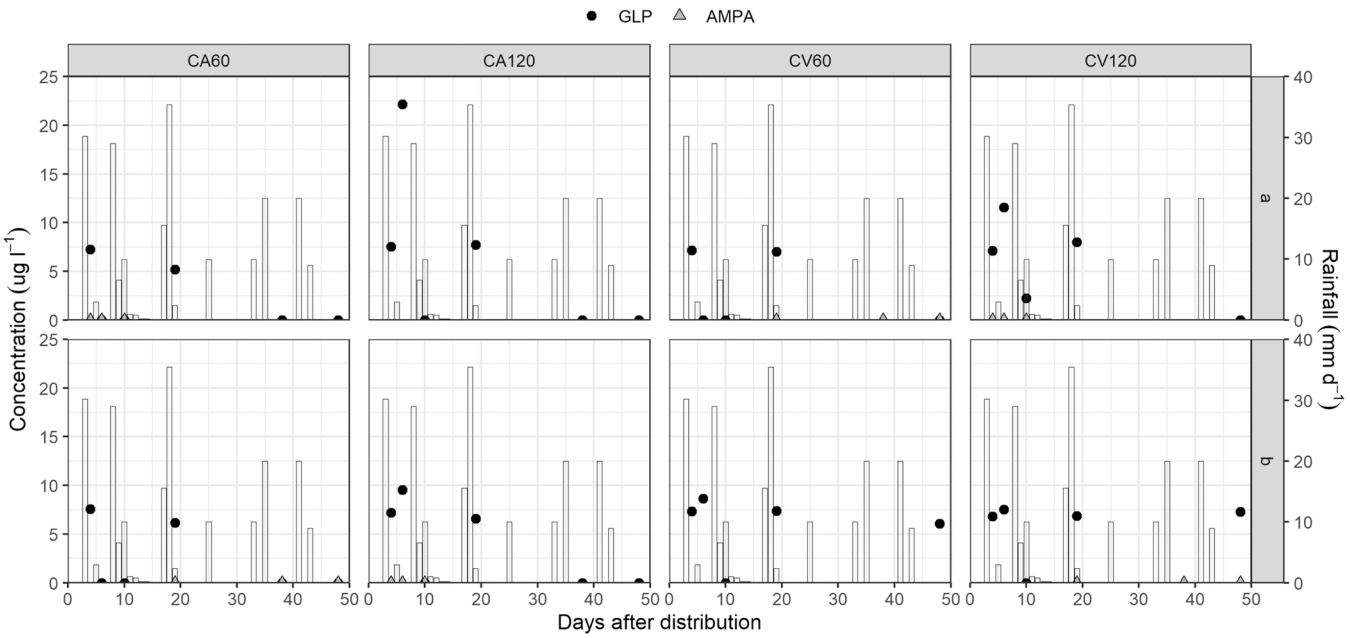

Fig. 5. GLP (black circles) and AMPA (grey triangles) concentration in groundwater for the eight studied lysimeters ("a" and "b" represent the two replicas). Bars refer to simulated rainfall amount (mm) during the sampling period.

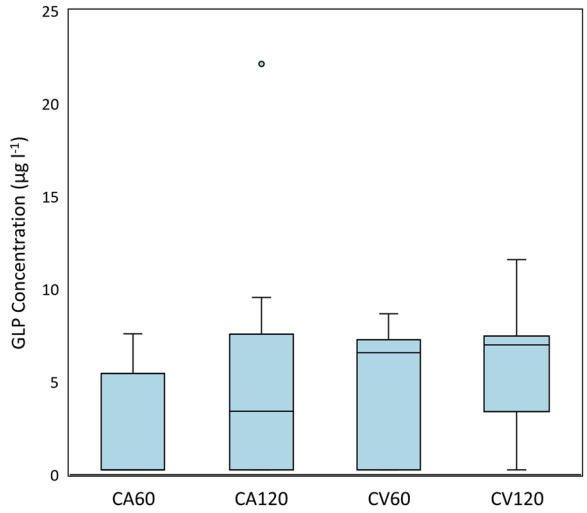

Fig. 6. Glyphosate concentration in groundwater for the four treatments. Middle lines refer to median values.

et al., 2021) due to a pronounced macropore structure, emphasizing the risk of groundwater contamination. When more time passed since the GLP application, further detection of GLP in soil and water showed different mobility according to the agricultural system and WT management. It is worth to note that in our experiment the surface water input did not differ between treatments (194 mm). Particularly, after 24 days GLP was detected at 30 and 60 cm depth only in WT60 (18.8 $\pm$ 11.8 and 7.1 $\pm$ 0.1 µg l^{-1} respectively), and once again on day 38 at concentrations of 6.7 $\pm$ 0.7 and 6.5 $\pm$ 0.4 µg l^{-1} at the same depths. In contrast, GLP concentration was < LOQ in WT120 at both depths on day 24, and only sporadically found on days 38 and 42. Mencaroni et al. (2021) found that under close-to-saturation conditions only the non-capillary macropores were empty, as in the surface layer of WT60. In such conditions, additional water input would converge part of water and solutes stored in the soil matrix into preferential pathway (Radolinski et al., 2022) by making the macropores more active (Krzeminska et al., 2014).

Consequently, the risk of fast movement and contamination may occur even in case of leaching events far from spraying application (Milan et al., 2022), especially when shallow water table conditions occur. When detected in the groundwater, GLP was found in WT60 up to 48 days after the application only in CV lysimeters (Fig. 5), and generally at concentrations much higher than the European drinking water limit (0.1 µg l^{-1}). Glyphosate was mostly found in concomitance of a high water input ($\geq$ 30 mm), which has increased the leaching transport of the molecule bypassing the porous matrix of the intermediate layers (Mencaroni et al., 2022). However, it must be noted that such intense rainfall events are not as common as usually monitored in the study area (Dal Ferro et al., 2017), emphasizing that GLP fast movement and findings in the groundwater might be partially overestimated. Moreover, this lysimeter study was a strictly controlled experiment avoiding water runoff, which could have affected the surface-groundwater repartition of the pesticide. However, we were not far from open-field conditions of the low-lying Venetian plain whose runoff losses are usually lower than 30 mm yr^{-1} (Morari et al., 2012), as well as the effect of water erosion negligible (Longo et al., 2021b). On the other hand, AMPA was seldom detected in the pore-water at 15 cm depth (Fig. 4), mostly in CV lysimeters, emphasizing a diverse occurrence between agricultural systems. Furthermore, AMPA had never reached the groundwater in all treatments, suggesting different adsorption and transport dynamics in soil compared to the parent molecule. This was likely due to the higher adsorption potential of AMPA than GLP towards soil (Sidoli et al., 2016) which might have reduced the mobility and in turn its transport through the soil matrix.

Regarding the dynamic in soil, in this study, dissipation rates were not estimated but concentrations of the herbicide found at the surface layer supported the hypothesis of a slightly faster dissipation of GLP under CA compared to CV management. For instance, it can be hypothesized that some additional bioavailable C input from crop residues under CA had likely enhanced GLP hydrolysis to sarcosine (la Cecilia and Maggi, 2018; Maggi et al., 2018). A minor amount of GLP reached the soil surface in the case of CA (−10%), due to the presence of rye which partially intercepted the spray. Besides the effect of crop interception, it is important to highlight that on day 18 in CA, on average, only 5 $\pm$ 1% of the initial amount of GLP was still detected in the surface

layer, compared to the 8 ± 1% left in CV. To note that GLP was < LOQ down to 15 cm after 42 days in CA (Table 5), but AMPA only occasionally. On the contrary, GLP and AMPA were still found in CV, suggesting faster mobility under conventional than conservation management. Furthermore, a faster AMPA formation was found at day 0 in CV compared to CA, likely due to the higher amount of GLP that reached the ground in bare soil and to a likely diverse contribution of the microbial degradation according to soil management (Habig and Swanepoel, 2015).

5. Conclusion

Our findings did not fully support the hypothesis that conservation practices during the transition period affected GLP dynamics in soil and water under shallow groundwater conditions. Indeed, GLP adsorption did not discriminate between different shallow water tables and agricultural systems, rather was the soil layering that modified GLP adsorption properties resulting to be mostly affected by clay fraction, SOC content, P Olsen and the presence of Al and Fe bonded to SOM. Neither two-year agricultural management nor long-term shallow water table conditions were effective drivers that did not modify the main physicochemical properties that affect adsorption. In contrast, the tested treatments affected dissipation and movement dynamics of both GLP and AMPA. Glyphosate transport through the soil profile was fast, with the likely formation of non-equilibrium preferential pathways that allowed GLP to bypass the soil matrix and directly reach the groundwater soon after its application. In particular, the shallower water table (WT60) increased the solute mobility down to the deepest layer. AMPA never reached the groundwater, being detected only at 15 cm depth. Despite differentiation between agricultural systems were still transitory and did not change the main soil properties, a higher dissipation of GLP and AMPA was found when conservation agriculture was adopted. It follows that the peculiar management conditions of CA, such as the occurrence of surface residues and a faster degradation in soil, might have mitigated the risk of groundwater contamination. Future studies are required to corroborate these results over a longer period of CA adoption and to investigate in depth the contribution of soil physicochemical properties and microbial populations in the GLP and AMPA dissipation dynamics.

CRediT authorship contribution statement

M. Mencaroni: Methodology, Data acquisition, Investigation, Writing – original draft. **M. Longo:** Methodology, Data acquisition, Investigation, Writing – review & editing. **A. Cardinali:** Methodology. **B. Lazzaro:** Funding, Writing – review & editing. **G. Zanin:** Conceptualization, Writing – review & editing. **N. Dal Ferro**: Supervision, Methodology, Writing – review & editing. **F. Morari:** Methodology, Funding acquisition, Supervision, Conceptualization, Writing – review & editing.

Declaration of Competing Interest

The authors declare that they have no known competing financial interests or personal relationships that could have appeared to influence the work reported in this paper.

Data Availability

Data will be made available on request.

Acknowledgments

This research was co-financed by the Rural Development Programme for Veneto 2014–2020. We would like to thank all the workers of the experimental farm “L. Toniolo” of the University of Padova for their support during the experimental set-up. A special thank goes to Federico Grillo for the help during the sampling campaign.

References

Accinelli, C., Koskinen, W.C., Seebinger, J.D., Vicari, A., Sadowsky, M.J., 2005. Effects of incorporated corn residues on glyphosate mineralization and sorption in soil. J. Agric. Food Chem. 53, 4110–4117. https://doi.org/10.1021/jf050186r.

Antier, C., Kudsk, P., Reboud, X., Ulber, L., Baret, P.V., Messéan, A., 2020. Glyphosate use in the European agricultural sector and a framework for its further monitoring. Sustain 12, 1–22. https://doi.org/10.3390/su12145682.

Autio, S., Siimes, K., Laitinen, P., Rämö, S., Oinonen, S., Eronen, L., 2004. Adsorption of sugar beet herbicides to Finnish soils. Chemosphere 55, 215–226. https://doi.org/10.1016/j.chemosphere.2003.10.015.

Basch, G., Friedrich, T., Kassam, A., Gonzalez-Sanchez, E., 2015. Conservation Agriculture in Europe. In: Farooq, M., Siddique, K. (Eds.), Conservation Agriculture. Springer, Cham, pp. 357–389.

Bascomb, C.L., 1968. Distribution of pyrophosphate-extractable iron and organic carbon in soils of various groups. J. Soil Sci.

Benbrook, C.M., 2016. Trends in glyphosate herbicide use in the United States and globally. Environ. Sci. Eur. 28, 1–15. https://doi.org/10.1186/s12302-016-0070-0.

Bento, C.P.M., Yang, X., Gort, G., Xue, S., van Dam, R., Zomer, P., Mol, H.G.J., Ritsema, C.J., Geissen, V., 2016. Persistence of glyphosate and aminomethylphosphonic acid in loess soil under different combinations of temperature, soil moisture and light/darkness. Sci. Total Environ. 572, 301–311. https://doi.org/10.1016/j.scitotenv.2016.07.215.

Bittelli, M., Andrenelli, M.C.C., Simonetti, G., Pellegrini, S., Artioli, G., Piccoli, I., Morari, F., 2019. Shall we abandon sedimentation methods for particle size analysis in soils? Soil Tillage Res 185, 36–46. https://doi.org/10.1016/j.still.2018.08.018.

Borggaard, O.K., Gimsing, A.L., 2008. Fate of glyphosate in soil and the possibility of leaching to ground and surface waters: a review 456, 441–456. https://doi.org/10.1002/ps.

Camarotto, C., Dal Ferro, N., Piccoli, I., Polese, R., Furlan, L., Chiarini, F., Morari, F., 2018. Conservation agriculture and cover crop practices to regulate water, carbon and nitrogen cycles in the low-lying Venetian plain. Catena 167, 236–249. https://doi.org/10.1016/j.catena.2018.05.006.

Candela, L., Álvarez-Benedí, J., Condesso de Melo, M.T., Rao, P.S.C., 2007. Laboratory studies on glyphosate transport in soils of the Maresme area near Barcelona, Spain: transport model parameter estimation. Geoderma 140, 8–16. https://doi.org/10.1016/j.geoderma.2007.02.013.

Carretta, L., Cardinali, A., Marotta, E., Zanin, G., Masin, R., 2019. A new rapid procedure for simultaneous determination of glyphosate and AMPA in water at sub μg/L level. J. Chromatogr. A. https://doi.org/10.1016/J.CHROMA.2019.04.047.

Carretta, L., Cardinali, A., Onofri, A., Masin, R., Zanin, G., 2021a. Dynamics of glyphosate and aminomethylphosphonic acid in soil under conventional and conservation tillage. Int. J. Environ. Res. https://doi.org/10.1007/s41742-021-00369-3.

Carretta, L., Masin, R., Zanin, G., 2021b. Review of studies analysing glyphosate and aminomethylphosphonic acid (AMPA) occurrence in groundwater. Environ. Rev. 1–22. https://doi.org/10.1139/er-2020-0106.

la Cecilia, D., Maggi, F., 2018. Analysis of glyphosate degradation in a soil microcosm. Environ. Pollut. 233, 201–207. https://doi.org/10.1016/J.ENVPOL.2017.10.017.

Chakraborty, P., Singh, N., Bansal, S., Sekaran, U., Sexton, P., Bly, A., Anderson, S.H., Kumar, S., 2022. Soil & tillage research does the duration of no-till implementation influence depth distribution of soil organic carbon, hydro-physical properties, and computed tomography-derived macropore characteristics ? Soil Tillage Res 222, 105426. https://doi.org/10.1016/j.still.2022.105426.

Clausen, L., Fabricius, I., Madsen, L., 2001. Adsorption of pesticides onto Quartz, Calcite, Kaolinite, and α-Alumina. J. Environ. Qual. 30, 846–857. https://doi.org/10.2134/jeq2001.303846x.

R. Core Team, 2017. R: A Language and Environment for Statistical Computing.

Cueff, S., Alletto, L., Bourdat-Deschamps, M., Benoit, P., Pot, V., 2020. Water and pesticide transfers in undisturbed soil columns sampled from a Stagnic Luvisol and a Vermic Umbrisol both cultivated under conventional and conservation agriculture. Geoderma 377, 114590. https://doi.org/10.1016/J.GEODERMA.2020.114590.

Dal Ferro, N., Zanin, G., Borin, M., 2017. Crop yield and energy use in organic and conventional farming: a case study in north-east Italy. Eur. J. Agron. 86, 37–47. https://doi.org/10.1016/j.eja.2017.03.002.

Dal Ferro, N., Camarotto, C., Piccoli, I., Berti, A., Mills, J., Morari, F., 2020. Stakeholder perspectives to prevent soil organic matter decline in northeastern Italy. Sustain 12, 1–18. https://doi.org/10.3390/su12010378.

De Gerónimo, E., Aparicio, V.C., 2021. Changes in soil pH and addition of inorganic phosphate affect glyphosate adsorption in agricultural soil. Eur. J. Soil Sci. 1–16. https://doi.org/10.1111/ejss.13188.

De Jonge, H., De Jonge, L.W., Jacobsen, O.H., Yamaguchi, T., Moldrup, P., 2001. Glyphosate sorption in soils of different pH and phosphorus content. Soil Sci. 166, 230–238. https://doi.org/10.1097/00010694-200104000-00002.

EFSA, 2015. Conclusion on the peer review of the pesticide risk assessment of the active substance glyphosate. EFSA J. 13. https://doi.org/10.2903/j.efsa.2015.4302.

FAO-UNESCO, 2008. Soil map of the world. Revised Legend.

Gerke, J., 2010. Humic (organic matter)-Al(Fe)-phosphate complexes: an underestimated phosphate form in soils and source of plant-available phosphate. Soil Sci. 175, 417–425. https://doi.org/10.1097/SS.0b013e3181f1b4dd.

Gilbert, R.O., 1988. Statistical methods for environmental pollution monitoring. Technometrics. https://doi.org/10.2307/1270090.

Gimsing, A.L., Borggaard, O.K., 2002. Effect of phosphate on the adsorption of glyphosate on soils, clay minerals and oxides. Int. J. Environ. Anal. Chem. 82, 545–552. https://doi.org/10.1080/0306731021000062964.
Glass, R.L., 1987. Adsorption of glyphosate by soils. J. Agric. Food Chem. 35, 497–500. https://doi.org/10.1002/ps.2780070407.
Haarstad, K., Ludvigsen, G.H., 2007. Ten years of pesticide monitoring in norwegian ground water. Gr. Water Monit. Remediat 27, 75–89. https://doi.org/10.1111/j.1745-6592.2007.00153.x.
Habig, J., Swanepoel, C., 2015. Effects of conservation agriculture and fertilization on soil microbial diversity and activity. Environ. - MDPI 2, 358–384. https://doi.org/10.3390/environments2030358.
Jarvis, N.J., 2007. A review of non-equilibrium water flow and solute transport in soil macropores: principles, controlling factors and consequences for water quality. Eur. J. Soil Sci. 71, 279–302. https://doi.org/10.1111/ejss.12973.
de Jonge, L.W., Kjaergaard, C., Moldrup, P., 2004. Colloids and colloid-facilitated transport of contaminants in soils: an introduction. Vadose Zo. J. 3, 321–325. https://doi.org/10.2113/3.2.321.
Khalil, Y., Flower, K., Siddique, K.H.M., Ward, P., 2018. Effect of crop residues on interception and activity of prosulfocarb, pyroxasulfone, and trifluralin. PLoS One 13, e0208274. https://doi.org/10.1371/JOURNAL.PONE.0208274.
Kjær, J., Ernsten, V., Jacobsen, O.H., Hansen, N., de Jonge, L.W., Olsen, P., 2011. Transport modes and pathways of the strongly sorbing pesticides glyphosate and pendimethalin through structured drained soils. Chemosphere 84, 471–479. https://doi.org/10.1016/j.chemosphere.2011.03.029.
Krzeminska, D.M., Bogaard, T.A., Debieche, T.H., Cervi, F., Marc, V., Malet, J.P., 2014. Field investigation of preferential fissure flow paths with hydrochemical analysis of small-scale sprinkling experiments. Earth Surf. Dyn. 2, 181–195. https://doi.org/10.5194/esurf-2-181-2014.
Kumari, N., Mohan, C., 2021. Basics of clay minerals and their characteristic properties. IntechOpen Clay C. https://doi.org/10.5772/intechopen.97672.
Laitinen, P., 2009. Fate of the organophosphate herbicide glyphosate in arable soils and its relationship to soil phosphorus status.
Locke, M.A., Zablotowicz, R.M., Bauer, P.J., Steinriede, R.W., Gaston, L.A., 2005. Conservation cotton production in the southern United States: herbicide dissipation in soil and cover crops. Weed Sci. 53, 717–727. https://doi.org/10.1614/ws-04-174r1.1.
Longo, M., Dal Ferro, N., Lazzaro, B., Morari, F., 2021b. Trade-offs among ecosystem services advance the case for improved spatial targeting of agri-environmental measures. J. Environ. Manag. 285, 112131 https://doi.org/10.1016/j.jenvman.2021.112131.
Longo, M., Jones, C.D., Izaurralde, R.C., Cabrera, M.L., Dal Ferro, N., Morari, F., 2021a. Testing the EPIC Richards submodel for simulating soil water dynamics under different bottom boundary conditions. Vadose Zo. J. 1–18. https://doi.org/10.1002/vzj2.20142.
Lutri, V.F., Matteoda, E., Blarasin, M., Aparicio, V., Giacobone, D., Maldonado, L., Becher Quinodoz, F., Cabrera, A., Giuliano Albo, J., 2020. Hydrogeological features affecting spatial distribution of glyphosate and AMPA in groundwater and surface water in an agroecosystem. Córdoba, Argentina. Sci. Total Environ. 711, 134557 https://doi.org/10.1016/j.scitotenv.2019.134557.
Maggi, F., Conoley, C., la Cecilia, D., Vervoort, R.W., Coleman, N.V., Tang, F.H.M., 2018. Glyphosate dispersion, degradation, and aquifer contamination in vineyards and wheat fields in the Po Valley, Italy. Water Res 146, 37–54. https://doi.org/10.1016/j.watres.2018.09.008.
McKeague J.A., Brydon J.E., Miles N.M., 1971. Differentiation of Forms of Extractable Iron and Aluminum in Soils 35, 33–38.
Mencaroni, M., Dal Ferro, N., Redcliffe, D., Morari, F., 2021. Preferential solute transport under variably saturated conditions in a silty loam soil: is the shallow water table a driving factor? J. Hydrol. 602 https://doi.org/10.1016/J.JHYDROL.2021.126733.
Mencaroni, M., Cardinali, A., Costa, L., Morari, F., Salandin, P., Zanin, G., Dal Ferro, N., 2022. Glyphosate and AMPA have low mobility through different soil profiles of the prosecco wine production area: a monitoring study in north-eastern Italy. Front. Environ. Sci. 10, 1525. https://doi.org/10.3389/FENVS.2022.971931/BIBTEX.
Milan, M., Vidotto, F., Fogliatto, S., 2022. Leaching of Glyphosate and AMPA from Field Lysimeters. Agronomy 12. https://doi.org/10.3390/agronomy12020328.
Morari, F., 2006. Drainage flux measurement and errors associated with automatic tension-controlled suction plates. Soil Sci. Soc. Am. J. 70, 1860. https://doi.org/10.2136/sssaj2006.0009.
Morari, F., Lugato, E., Polese, R., Berti, A., Giardini, L., 2012. Nitrate concentrations in groundwater under contrasting agricultural management practices in the low plains of Italy. Agric. Ecosyst. Environ. 147, 47–56. https://doi.org/10.1016/j.agee.2011.03.001.
Morillo, E., Undabeytia, T., Maqueda, C., Ramos, A., 2000. Glyphosate adsorption on soils of different characteristics. Influ. Copp. Addit. Chemosphere 40, 103–107. https://doi.org/10.1016/S0045-6535(99)00255-6.
Munira, S., Farenhorst, A., Flaten, D., Grant, C., 2016. Phosphate fertilizer impacts on glyphosate sorption by soil. Chemosphere 153, 471–477. https://doi.org/10.1016/j.chemosphere.2016.03.028.
OECD, 2000. OECD 106 Adsorption - Desorption Using a Batch Equilibrium Method. Test. Chem. OECD, Guidel, pp. 1–44. https://doi.org/10.1787/9789264069602-en.
Okada, E., Costa, J.L., Bedmar, F., Barbagelata, P., Irizar, A., Rampoldi, E.A., 2014. Effect of conventional and no-till practices on solute transport in long term field trials. Soil Tillage Res 142, 8–14. https://doi.org/10.1016/j.still.2014.04.002.
Okada, E., Costa, J.L., Bedmar, F., 2016. Adsorption and mobility of glyphosate in different soils under no-till and conventional tillage. Geoderma 263, 78–85. https://doi.org/10.1016/j.geoderma.2015.09.009.
Okada, E., Costa, J.L., Bedmar, F., 2019. Glyphosate DiSsipation in Different Soils under No-till and Conventional tillage. Pedosphere 29, 773–783. https://doi.org/10.1016/S1002-0160(17)60430-2.
Ololade, I.A., Oladoja, N.A., Oloye, F.F., Alomaja, F., Akerele, D.D., Iwaye, J., Aikpokpodion, P., 2014. Sorption of glyphosate on soil components: the roles of metal oxides and organic materials. Soil Sediment Contam. Int. J. 23, 571–585. https://doi.org/10.1080/15320383.2014.846900.
Page, K.L., Dang, Y.P., Dalal, R.C., 2020. The ability of conservation agriculture to conserve soil organic carbon and the subsequent impact on soil physical, chemical, and biological properties and yield. Front. Sustain. Food Syst. 4, 1–17. https://doi.org/10.3389/fsufs.2020.00031.
Patle, G.T., Bandyopadhyay, K.K., Singh, D.K., 2013. Impact of conservation agriculture and resource conservation technologies on carbon sequestration - A review. Indian. J. Agric. Sci. 83, 3–13.
Pazikowska-Sapota, G., Galer-Tatarowicz, K., Dembska, G., Wojtkiewicz, M., Duljas, E., Pietrzak, S., Dzierzbicka-Glowacka, L.A., 2020. The impact of pesticides used at the agricultural land of the Puck commune on the environment of the Puck Bay. PeerJ 2020, 1–21. https://doi.org/10.7717/peerj.8789.
Piccoli, I., Chiarini, F., Carletti, P., Furlan, L., Lazzaro, B., Nardi, S., Berti, A., Sartori, L., Dalconi, M.C., Morari, F., 2016. Disentangling the effects of conservation agriculture practices on the vertical distribution of soil organic carbon. Evidence of poor carbon sequestration in North- Eastern Italy. Agric., Ecosyst. Environ. 230, 68–78. https://doi.org/10.1016/j.agee.2016.05.035.
Piccoli, I., Camarotto, C., Lazzaro, B., Furlan, L., Morari, F., 2017. Conservation agriculture had a poor impact on the soil porosity of Veneto low-lying plain silty soils after a 5-year transition period. L. Degrad. Dev. 28, 2039–2050. https://doi.org/10.1002/ldr.2726.
Piccolo, A., Celano, G., Arienzo, M., Mirabella, A., 1994. Adsorption and desorption of glyphosate in some eropean soils.
Pizzeghello, D., Berti, A., Nardi, S., Morari, F., 2011. Phosphorus forms and P-sorption properties in three alkaline soils after long-term mineral and manure applications in north-eastern Italy. Agric. Ecosyst. Environ. 141, 58–66. https://doi.org/10.1016/j.agee.2011.02.011.
Prata, F., Lavorenti, A., Regitano, J.B., 2005. Seção Ii - Química E Mineralogia Do Solo Glyphosate Behavior in a Rhodic Oxisol Under No-Till and Conventional 61–69.
Radolinski, J., Le, H., Hilaire, S.S., Xia, K., Scott, D., Stewart, R.D., 2022. A spectrum of preferential flow alters solute mobility in soils. Sci. Rep. 12, 1–11. https://doi.org/10.1038/s41598-022-08241-w.
Sidoli, P., Baran, N., Angulo-Jaramillo, R., 2016. Glyphosate and AMPA adsorption in soils: laboratory experiments and pedotransfer rules. Environ. Sci. Pollut. Res. 23, 5733–5742. https://doi.org/10.1007/s11356-015-5796-5.
Silburn, D.M., 2020. Pesticide retention, degradation, and transport off-farm. No-till Farming Syst. Sustain. Agric 281–297. https://doi.org/10.1007/978-3-030-46409-7_17.
Sprankle, P., Meggitt, W.F., Penner, D., 1975. Adsorption, mobility, and microbial degradation of glyphosate in the soil. Weed Sci. https://doi.org/10.1017/s0043174500052929.
Székács, A., Mörtl, M., Darvas, B., 2015. Monitoring Pesticide Residues in Surface and Ground Water in Hungary: Surveys in 1990–2015, 2015 J. Chem.. https://doi.org/10.1155/2015/717948.
U.S. EPA, 1993. Reregistration Eligibility Decision (RED) Glyphosate.
Wahl, N.A., Bens, O., Buczko, U., Hangen, E., Hüttl, R.F., 2004. Effects of conventional and conservation tillage on soil hydraulic properties of a silty-loamy soil. Phys. Chem. Earth,Parts A/B/C 29, 821–829. https://doi.org/10.1016/J.PCE.2004.05.009.